Ocean Engineering 2008, Vol. 35, No. 2, pp. 191-200.

Slender-Body Methods for Predicting Ship Squat

Tim Gourlay
Centre for Marine Science and Technology, Curtin University

Abstract

A review is made of linear slender-body methods for predicting the squat of a ship in shallow open water, dredged channels or canals. The results are summarized into a general formula based on Fourier transforms, and the method is extended to cater to stepped canals. An approximate solution for canals of arbitrary cross-section is proposed.

1. Introduction

Thin-ship methods have been used for predicting the wave resistance of ships since Michell (1898). These formulations assume that the ship's beam is small compared to its length, in which case generated wave amplitudes are also small compared to the ship's length. This allows linearization of the free surface boundary condition, and a series solution in increasing powers of the beam/shiplength (B/L) ratio. Usually the ship draft is also small compared to the ship length, further reinforcing the assumption of small free surface displacements, and allowing the flow to be computed using slender-body theory (Tuck 1964).

For a slender ship moving in shallow water, the water depth may also be small compared to the shiplength. In this case the flow becomes essentially two-dimensional, with horizontal flow velocities dominating over vertical flow velocities. Solution of the leading-order flow is then simplified. Tuck (1966) solved the leading-order flow around a slender ship in shallow open water of constant depth. Although this leading-order solution could not be used to calculate wave resistance, it was able to calculate dynamic sinkage and trim, except when the ship speed was close to the "critical" speed of long waves in shallow water ($=\sqrt{gh}$, with g = gravitational acceleration, h = water depth).

Since 1966, linear slender-body shallow-water theory has been extended to various bottom topographies, including both steady and unsteady flow. Nonlinear terms have been included in the formulation for narrow channels, and higher-order terms have been included for transcritical flow.

In this article we shall be considering only linear first-order theories. Such methods are best suited to long, slender hulls such as large high-speed catamaran demihulls ($B/L \approx 0.05-0.10$) or frigates and destroyers ($B/L \approx 0.10-0.12$). However the methods have also been successfully used to predict the squat of containerships ($B/L \approx 0.11-0.15$) and even capesize bulk carriers ($B/L \approx 0.16-0.20$).

We shall be concentrating on the case of steady "subcritical" flow, which is of most interest to mariners. In the 1960s and 1970s, this flow was solved for various bottom topographies, namely:

- open water, constant depth (Tuck 1966)
- canal of constant depth and width (Tuck 1967)
- dredged channel with constant depth in the inner and outer regions (Beck et al 1975)

Here we shall summarize these results and rewrite them in a form which is more applicable to modern transom-stern ships. We shall also provide results for another bottom topography, and discuss extension of the method to a canal of arbitrary cross-section.

2. Open water of constant depth

For a ship moving in open shallow water of constant depth, Tuck (1966) showed that the ship can be modelled as a line of sources and sinks, with sources forcing the flow outwards where the ship's section area is increasing towards the stern, and sinks pulling the flow inwards where the section area is decreasing towards the stern.

Specifically, if we consider a ship-fixed coordinate system with longitudinal coordinate x centred at midships (positive towards the stern) and transverse coordinate y centred on the ship centreline (positive to starboard), the leading-order disturbance velocity potential ϕ satisfies the partial differential equation

$$\left(1-F_h^2\right)\frac{\partial^2\phi}{\partial x^2}+\frac{\partial^2\phi}{\partial y^2}=0 \qquad (1)$$

Here F_h is the depth-based Froude number $U/\sqrt{gh}$, with U the free stream speed (equal to the ship speed in earth-fixed coordinates). For subcritical flow, such as we are considering here, $F_h<1$ and equation (1) is an elliptic partial differential equation. It is subject to the inner boundary condition

$$\frac{\partial\phi}{\partial y}=\pm\frac{U}{2h}S'(x) \text{ on } y=0_{\pm} \qquad (2)$$

where $S(x)$ is the hull cross-sectional area at position x, and the prime denotes the derivative dS/dx. We also have the far-field boundary condition

$$\frac{\partial\phi}{\partial x},\frac{\partial\phi}{\partial y}\to 0 \text{ as } y\to\pm\infty \qquad (3)$$

By considering the velocity potential for a line of moving sources, and choosing the source strengths so that equation (2) is satisfied, Tuck found expressions for the velocity potential and resulting pressure field, involving direct integration of a singular integral.

Here we give an alternative solution which uses Fourier transforms rather than source summation. By taking the Fourier transform of equation (1) and solving subject to boundary condition (2), the velocity potential may be written in the form

$$\phi=-\frac{U}{4\pi h\sqrt{1-F_h^2}}\int_{-\infty}^{\infty}\frac{\overline{S'}(k)}{|k|}\,e^{-\sqrt{1-F_h^2}|k|y}\,e^{-ikx}\,dk \qquad (4)$$

We have directly used the Fourier transform of the derivative of the section area, namely

$$\overline{S'}(k) = \int_{-\infty}^{\infty} S'(x)\, e^{ikx} dx \tag{5}$$

Hydrodynamic pressure, vertical force and trim moment can now be calculated as in Tuck (1966). For example, the upwards vertical force Z on a ship which is held vertically at its static draft and trim is

$$Z = -\frac{\rho U^2}{4\pi h\sqrt{1-F_h^2}} \int_{-\infty}^{\infty} i\, \overline{S'}(k)\, \overline{B^*}(k) \operatorname{sgn}(k)\, dk \tag{6}$$

Here $\overline{B}(k)$ denotes the Fourier transform of $B(x)$, and the asterisk denotes complex conjugate. The bow-down trim moment is found by replacing $\overline{B}(k)$ by $\overline{xB}(k)$, where $\overline{xB}(k)$ is the Fourier transform of $xB(x)$.

The Fourier integral representation (6) provides an alternative method for calculating the vertical force and trim moment, with the computational advantage of having a non-singular integrand. Once the vertical force and trim moment have been computed, the sinkage and trim then follow hydrostatically, as described in Tuck (1966).

3. Canal of constant depth and width

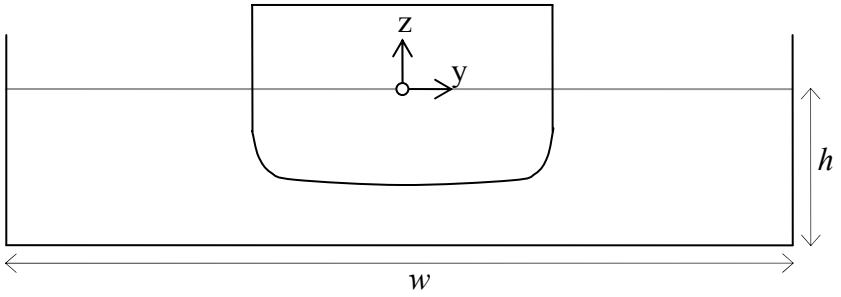

Figure 1: Cross-section through a ship in a canal of constant depth and width

Figure 1 shows a cross-section through a ship in a canal of constant depth and width, looking from ahead of the ship. The ship is taken to be moving along the centreline of the canal, so that no cross-flow occurs. In this case, the governing partial differential equation (1) and hull boundary condition (2) still apply. The far-field boundary condition used in open water is replaced by a wall boundary condition.

This problem was solved by Tuck (1967) using Fourier transforms. It was found that the percentage increase in midship sinkage from open water to a rectangular canal was governed by the quantity $\frac{w}{L}\sqrt{1-F_h^2}$, where L is the ship's waterline length. Therefore increasing the ship speed amplifies the effect of finite channel width on squat.

The method used in Tuck (1967) involved integrating the hull boundary condition (2) by parts, and applying the assumption of zero section area at the bow and stern. For modern transom stern ships, this assumption would require the flow to "bang shut"

immediately behind the transom. When the ship is travelling fast enough for flow to detach smoothly from the transom, a better method may be to use the hull boundary condition (2) in its original form, setting $S'(x) = 0$ ahead of and behind the ship. Therefore the Fourier transform is calculated using equation (5) over the wetted length of the ship. This models the ship as having zero section area ahead of the bow, its usual section area over its wetted length, and a transom that extends downstream to infinity with constant cross-section. This method ensures smooth flow detachment from the transom.

Re-deriving the solution, without the assumption of zero section area at the stern, yields the alternative solution valid for both cruiser and transom sterns:

$$Z = -\frac{\rho U^2}{4\pi h\sqrt{1-F_h^2}} \int_{-\infty}^{\infty} i\,\overline{S'}(k)\,\overline{B^*}(k)\,\coth\left(\tfrac{w}{2}\sqrt{1-F_h^2}\,k\right)dk \qquad (7)$$

Again, a similar expression exists for the trim moment, and sinkage and trim follow from hydrostatics.

4. Dredged channel

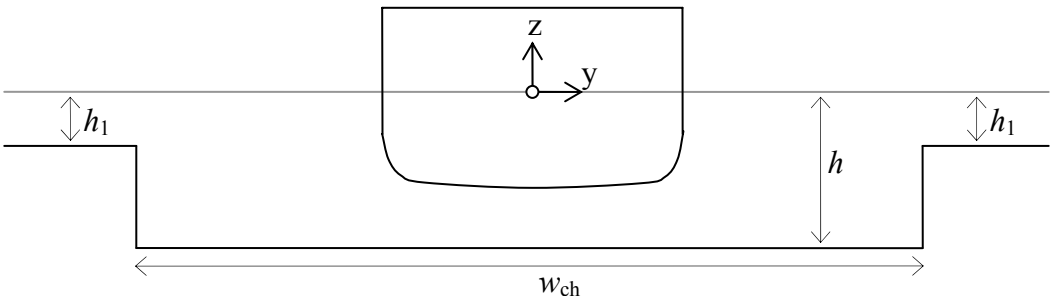

Figure 2: Cross-section through a ship in a dredged channel with constant inner and outer depths

Figure 2 shows a ship in a dredged channel, with the dredged channel and the area either side each having constant depth. Again, the ship is taken to be moving along the centreline of the channel.

This problem was solved by Beck et al (1975) using Fourier transforms. They used the same partial differential equation (1) and hull boundary condition (2), and matched the velocity potential ϕ and transverse flux $h\frac{\partial\phi}{\partial y}$ on each side of the step depth continuity. Again, the assumption of zero section area at the ship's stern was applied, making the method less applicable to modern transom-stern ships.

Re-derivation of the solution using the derivative of the section area yields, using the present notation,

$$Z = -\frac{\rho U^2}{4\pi h\sqrt{1-F_h^2}} \int_{-\infty}^{\infty} i\,\overline{S'}(k)\,\overline{B^*}(k)\,K(k)\,dk \qquad (8)$$

The function $K(k)$ is given by

$$K(k) = \frac{\cosh\left(\frac{w_{ch}}{2}\sqrt{1-F_h^2}\,k\right) + \frac{h_1\lambda}{h\sqrt{1-F_h^2}\,k}\sinh\left(\frac{w_{ch}}{2}\sqrt{1-F_h^2}\,k\right)}{\sinh\left(\frac{w_{ch}}{2}\sqrt{1-F_h^2}\,k\right) + \frac{h_1\lambda}{h\sqrt{1-F_h^2}\,k}\cosh\left(\frac{w_{ch}}{2}\sqrt{1-F_h^2}\,k\right)} \tag{9}$$

Here $\lambda^2 = \left(1-F_1^2\right)k^2$, with $F_1 = U/\sqrt{gh_1}$. The sign of λ must be chosen so that the far-field solution either tends towards zero when the outer flow is subcritical ($F_1 \le 1$), or represents outgoing rather than incoming waves when the outer flow is supercritical ($F_1 \ge 1$). These requirements yield

$$\lambda = \begin{cases} \sqrt{1-F_1^2}\,|k| & F_1 < 1 \\ -i\sqrt{F_1^2-1}\;k & F_1 > 1 \end{cases} \tag{10}$$

Note that for the special case when $F_1 = 1$, we have

$$K(k) = \coth\left(\frac{w_{ch}}{2}\sqrt{1-F_h^2}\,k\right) \tag{11}$$

This yields the same result as for the canal described in Section 3, with $w_{ch} = w$. Therefore if the ship is travelling at such a speed that the flow outside the channel is critical, the flow within the channel is the same as if the ship were in a wall-sided canal of the same width. This is because when flow outside the channel is critical, there is zero transverse flux out of the channel, the same as for a canal.

5. Stepped canal

Here we shall develop a general solution for a stepped canal, which will later be used to estimate the sinkage and trim of a ship in a channel of arbitrary cross-section.

The geometry of this situation is shown in Figure 3. The channel configuration is assumed symmetrical, with the ship moving along the centreline.

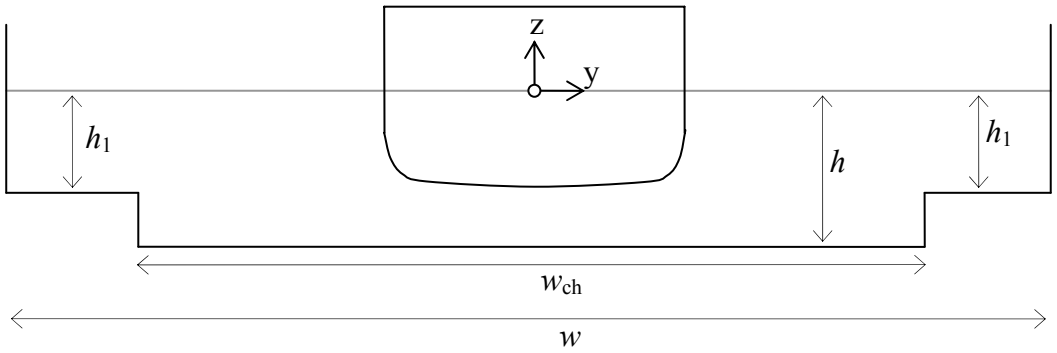

Figure 3: Cross-section through a ship in a symmetric canal with an arbitrary step depth change

This flow satisfies the following equations:
- Laplace's equation (equation 1)
- Modified hull boundary condition (equation 2)
- Wall boundary condition at sides of canal

$$\frac{\partial \phi}{\partial y} = 0 \text{ on } y = \pm \tfrac{w}{2} \tag{12}$$

- Continuity of free surface height across the step depth change, through continuity of the velocity potential ϕ.

- Continuity of transverse flux $h\frac{\partial \phi}{\partial y}$ across the step depth change.

Since the flow is symmetric about $y = 0$, we shall consider only the region $y > 0$. In the channel region $0 \le y \le w_{ch}/2$, the Fourier-transformed Laplace's equation is

$$\frac{\partial^2 \bar{\phi}}{\partial y^2} = k^2\left(1 - F_h^2\right)\bar{\phi} \tag{13}$$

Together with the hull boundary condition (2), this has the general solution

$$\bar{\phi} = \frac{U\bar{S}'(k)}{2hk\sqrt{1-F_h^2}}\sinh\left(\sqrt{1-F_h^2}ky\right) + A(k)\cosh\left(\sqrt{1-F_h^2}ky\right) \tag{14}$$

In the outer region $w_{ch}/2 \le y \le w/2$, equation (13) is also applicable, with h_1 replacing *h*. Combining this with the wall boundary condition (12), the general solution in the outer region is

$$\bar{\phi} = B(k)\cosh\left[\lambda\left(y - \frac{w}{2}\right)\right] \tag{15}$$

Again, $\lambda^2 = \left(1 - F_1^2\right)k^2$, however for the canal the sign of λ is immaterial since equation (15) is even in λ.

Matching $\bar{\phi}$ at $y = w_{ch}/2$ yields

$$\frac{U\bar{S}'(k)}{2hk\sqrt{1-F_h^2}}\sinh\left(\frac{w_{ch}}{2}\sqrt{1-F_h^2}k\right) + A(k)\cosh\left(\frac{w_{ch}}{2}\sqrt{1-F_h^2}k\right) = B(k)\cosh\left[\lambda\left(\frac{w_{ch}-w}{2}\right)\right] \tag{16}$$

Matching $h\frac{\partial \bar{\phi}}{\partial y}$ at $y = w_{ch}/2$ yields

$$\frac{U\bar{S}'(k)}{2}\cosh\left(\frac{w_{ch}}{2}\sqrt{1-F_h^2}k\right) + A(k)\sqrt{1-F_h^2}kh\sinh\left(\frac{w_{ch}}{2}\sqrt{1-F_h^2}k\right) = h_1\lambda B(k)\sinh\left[\lambda\left(\frac{w_{ch}-w}{2}\right)\right] \tag{17}$$

Solving equations (16,17) simultaneously gives

$$A(k) = -\frac{U\overline{S'}(k)}{2h\sqrt{1-F_h^2 k}} \left\{ \frac{\cosh\left(\frac{w_{ch}}{2}\sqrt{1-F_h^2 k}\right) + \frac{h_1\lambda}{h\sqrt{1-F_h^2 k}}\sinh\left(\frac{w_{ch}}{2}\sqrt{1-F_h^2 k}\right)\tanh\left(\lambda\left(\frac{w-w_{ch}}{2}\right)\right)}{\sinh\left(\frac{w_{ch}}{2}\sqrt{1-F_h^2 k}\right) + \frac{h_1\lambda}{h\sqrt{1-F_h^2 k}}\cosh\left(\frac{w_{ch}}{2}\sqrt{1-F_h^2 k}\right)\tanh\left(\lambda\left(\frac{w-w_{ch}}{2}\right)\right)} \right\} \tag{18}$$

Equation (14) is now inverted to find the velocity potential, whereupon the vertical force becomes

$$Z = \frac{\rho U}{2\pi}\int_{-\infty}^{\infty} i\,k\;A(k)\;\overline{B^*}(k)\,dk \tag{19}$$

This can be written

$$Z = -\frac{\rho U^2}{4\pi h\sqrt{1-F_h^2}}\int_{-\infty}^{\infty} i\;\overline{S'}(k)\;\overline{B^*}(k)\;K(k)\,dk \tag{20}$$

where

$$K(k) = \frac{\cosh\left(\frac{w_{ch}}{2}\sqrt{1-F_h^2 k}\right) + \frac{h_1\lambda}{h\sqrt{1-F_h^2 k}}\sinh\left(\frac{w_{ch}}{2}\sqrt{1-F_h^2 k}\right)\tanh\left(\lambda\left(\frac{w-w_{ch}}{2}\right)\right)}{\sinh\left(\frac{w_{ch}}{2}\sqrt{1-F_h^2 k}\right) + \frac{h_1\lambda}{h\sqrt{1-F_h^2 k}}\cosh\left(\frac{w_{ch}}{2}\sqrt{1-F_h^2 k}\right)\tanh\left(\lambda\left(\frac{w-w_{ch}}{2}\right)\right)} \tag{21}$$

As for the dredged channel, when flow in the outer region is critical ($F_1 = 1$), the flow within the channel is identical to that of a rectangular canal with width equal to the channel width.

6. Numerical calculations

As an example of these calculations, consider a MarAd L-series bulk carrier (Roseman 1987) at level static trim and beam/draft ratio of 4.4. This ship is travelling in water with the following transverse geometries:

Configuration	**Example dimensions**
Open water	valid for all $h << L$
Rectangular canal	$w/L = 1.0$, valid for all $h << L$
Dredged channel	$w_{ch}/L = 1.0$, $h_1/h = 0.50$, valid for all $h << L$
Stepped canal	$w_{ch}/L = 1.0$, $w/L = 2.0$, $h_1/h = 0.50$, valid for all $h << L$

Calculated sinkage for these example cases is shown in Figure 4. The sinkage coefficient c_s is defined by

$$s_{LCF} = c_s \frac{\nabla}{L^2}\frac{F_h^2}{\sqrt{1-F_h^2}} \tag{22}$$

where s_{LCF} is the sinkage at the longitudinal centre of floatation, and ∇ is the ship's displaced volume. This sinkage coefficient is used because it is predicted to be constant in open water, according to slender-body theory.

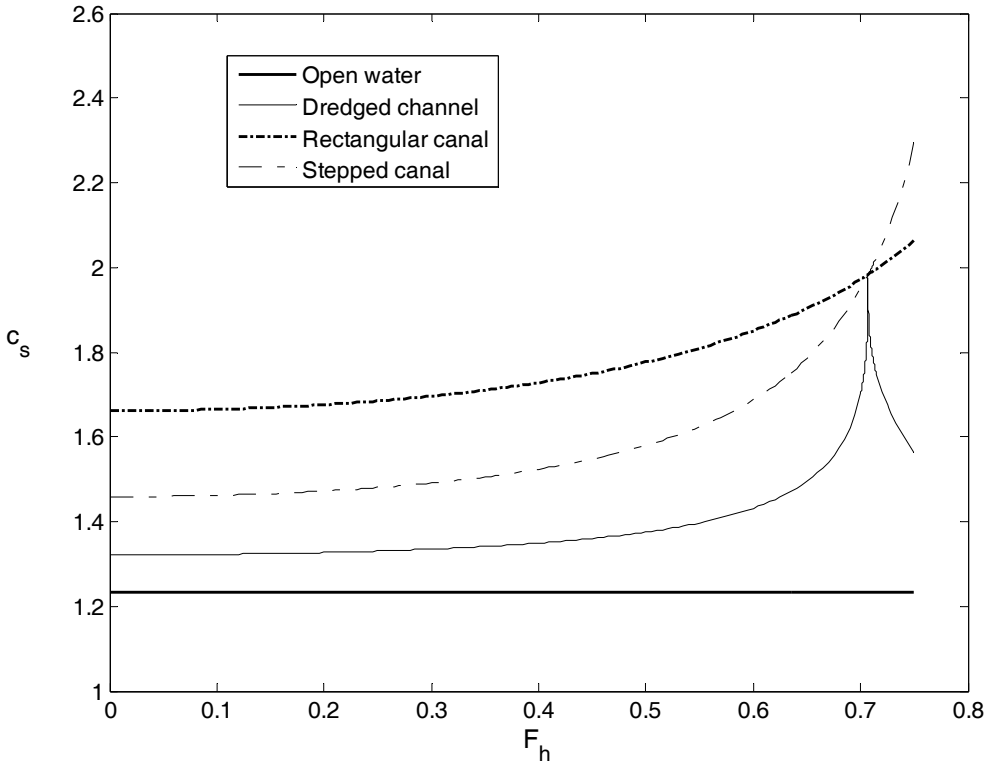

Figure 4: Calculated LCF sinkage coefficients for various example channel configurations

Points to note from Figure 4 include:

- The channel and canal sinkage coefficients are all larger than the open-water value, by an amount which depends on the geometry; these coefficients also vary with F_h.
- The dredged channel and stepped canal results both have critical flow in the outer region at $F_h = 0.707$. Since the flow is critical, there is zero transverse flux out of the channel, and the channel behaves like a surface-piercing wall. Therefore the results coincide with the rectangular canal results at this point.
- The dredged channel results are "cusped" when flow becomes critical in the outer region. This is because the depth change outside the channel generally exerts only a small influence on the ship squat, however a singularity occurs when the outer flow becomes critical. In this case the flow must match the canal flow according to linear theory, and the critical flow occurs over an infinite domain (from the edge of the channel out to infinity). A similar singularity occurs in open water at the critical speed. In both cases, nonlinearity and dispersion act to smooth the sinkage as a function of F_h. Sample calculations have been done including the leading-order effect of dispersion in the outer region, similar to the transcritical method described in Gourlay & Tuck (2001). Dispersion was seen to decrease and broaden the peak slightly.

The trim coefficient c_θ is defined analogously to the sinkage coefficient, with θ the change in bow-down trim angle in radians:

$$\theta = c_\theta \frac{\nabla}{L^3} \frac{F_h^2}{\sqrt{1-F_h^2}} \tag{23}$$

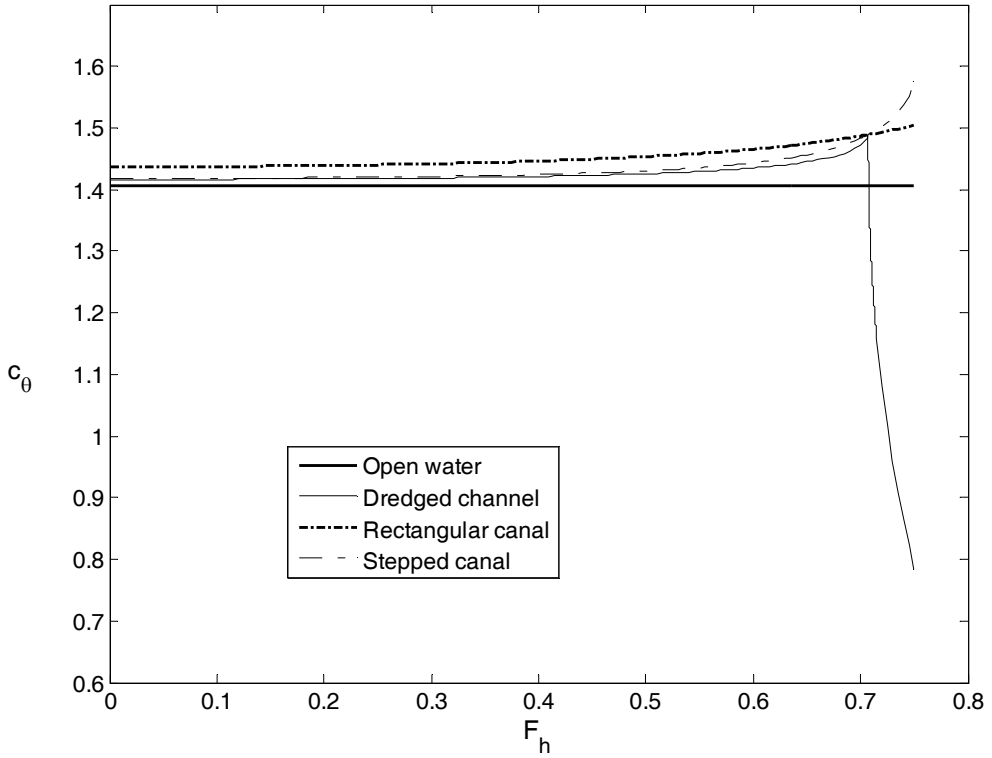

Figure 5: Calculated bow-down trim coefficients for various example channel configurations

Figure 5 shows the calculated trim coefficient for the same example cases. We see that the trim coefficient is approximately constant for all of the different channel configurations. This is true up until supercritical flow occurs outside the channel, in which case the channel geometry affects the trim markedly.

7. Effect of self-propulsion, viscosity and nonlinearity

The methods used in this article neglect self-propulsion, viscosity and nonlinearity, so it is appropriate to comment on the qualitative effect these have on sinkage and trim.

Self-propulsion creates a low-pressure region ahead of the propeller, which increases the sinkage slightly, and decreases the bow-down trim significantly. This effect was observed experimentally by Dand & Ferguson (1973), by comparing the sinkage and trim of towed and self-propelled models.

Viscosity is important within a boundary layer next to the ship's hull. This boundary layer is generally thin, but increases in thickness towards the stern. The character of the boundary layer is very different between model scale and full scale. At full scale (high Reynolds number), the boundary layer is naturally turbulent, thin compared to

the ship dimensions, stays reasonably well attached, and exerts little influence on the pressures on the hull. At model scale (low Reynolds number), the boundary layer is artificially tripped to become turbulent, is thick compared to the ship dimensions, more likely to separate near the stern, and may markedly change the hull pressure near the stern.

Self-propulsion also has the effect of re-energizing the boundary layer near the ship's stern, so that separation is less likely at full scale and especially at model scale. Therefore, when self-propulsion is taken into account, there is better correlation between model-scale and full-scale sinkage and trim (Dand & Ferguson 1973).

When the underkeel clearance is small, it is conceivable that viscous effects beneath the ship may affect sinkage and trim. However it was found in Gourlay (2006) that there is very little "blockage" effect due to the constriction beneath the hull. Instead, flow is simply diverted around the sides of the ship, causing a normal Bernoulli pressure drop on the sides of the ship, which then governs the pressure beneath the ship. Experimental sinkage and trim results showed no distinct "small-UKC" effect, beyond the normal increase due to decreased water depth.

Nonlinearity should not significantly affect the sinkage and trim for slender ships such as frigates, however for containerships and bulk carriers it becomes increasingly important. The linear solution uses only the leading-order dynamic free surface boundary condition, assuming free surface displacements to be small. Higher-order terms for calculating the flow around a ship in a wall-sided canal have been included by Sharma & Chen (2000). Also, according to linear theory the ship is fixed in its rest position for calculating the flow, and then hydrostatic balancing is used to calculate sinkage and trim. In reality the sinkage increases the immersed volume of the ship, further disturbing the flow and increasing the sinkage. This effect was studied by Gourlay (2000) for ships in narrow canals.

The towed model test results shown in Gourlay (2006) can be compared with the correct theoretical results for that canal, i.e. $c_s = 1.36$ and $c_\theta = 1.41$. This shows that, for the MarAd L-Series hull, experimental LCF sinkage is 3 – 26% larger than that predicted, over a range of speeds and water depths. This is attributed to the neglect of nonlinear terms which are important for bulk carriers. In practice, the LCF sinkage coefficient can be tuned to better match the model test results. Bow-down trim is 13 – 57% lower than that predicted, which is attributed to flow separation and decreased stern pressure at model scale. Theoretical trim results should be adjusted for the effect of self-propulsion in order to predict full-scale values.

8. Approximate solution for a canal of arbitrary cross-section

Here we shall develop an approximate method for calculating the sinkage and trim of a ship in a channel of arbitrary cross-section, by approximating the cross-sectional shape as two regions of constant depth joined by a step depth change.

As seen in equation (7), slender-body theory predicts that channel width and depth are both independently important in a rectangular canal, and that increasing the ship speed amplifies the effect of finite channel width on squat.

For a non-rectangular channel, we might expect that waterline width, cross-sectional area, and depth at the ship will be the most important factors governing the sinkage and trim. Waterline width couples with free surface deformation to govern flow continuity, and the effect of waterline width becomes increasingly important at higher Froude numbers, as the disturbance due to the ship spreads out further in the transverse direction. Decreasing cross-sectional area causes a blockage effect and tends to accelerate the flow. Having a larger water depth near the ship decreases the longitudinal flow speeds past the ship, diluting the hydrodynamic pressure and decreasing the squat.

In order to gauge whether waterline width, cross-sectional area, and depth at the ship are the most important factors governing squat of a ship in a channel of arbitrary cross-section, we can use the results of Section 5 to do a sensitivity analysis on channels with different cross-sections.

Consider the three channel configurations shown in Figure 6. Each of these is a stepped depth change as depicted in Figure 3, but all three are overlaid in the same diagram.

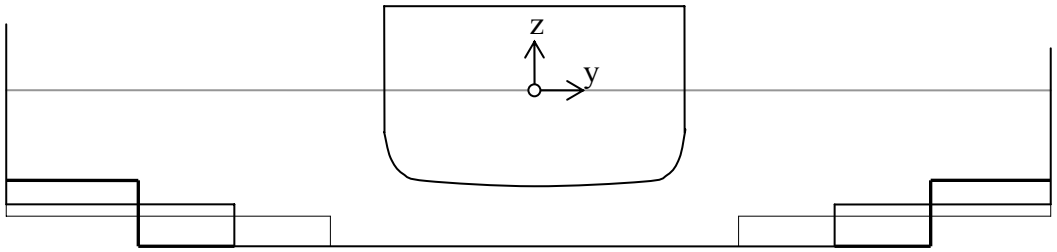

Figure 6: Overlay of three different step depth change channel cross-sections, used for sensitivity study

The three channel configurations all have the same waterline width, same cross-sectional area, and same depth near the ship. We can calculate the squat of all three channel configurations, with the following example conditions in dimensionless form:

Waterline channel width to ship waterline length ratio w/L	1.0
Inner channel width to waterline channel width ratio w_{ch}/w	0.4, 0.6, 0.8
Ratio of channel cross-sectional area to enclosing rectangle area	0.85
Ship type	MarAd L-series bulk carrier (Roseman 1987)

Note that, for $w_{ch}/w = 0.8$, the flow is supercritical in the outer region for $F_h \geq 0.5$.

For comparison, results for a rectangular canal with the same cross-sectional area have also been calculated. Results are shown in Figure 7.

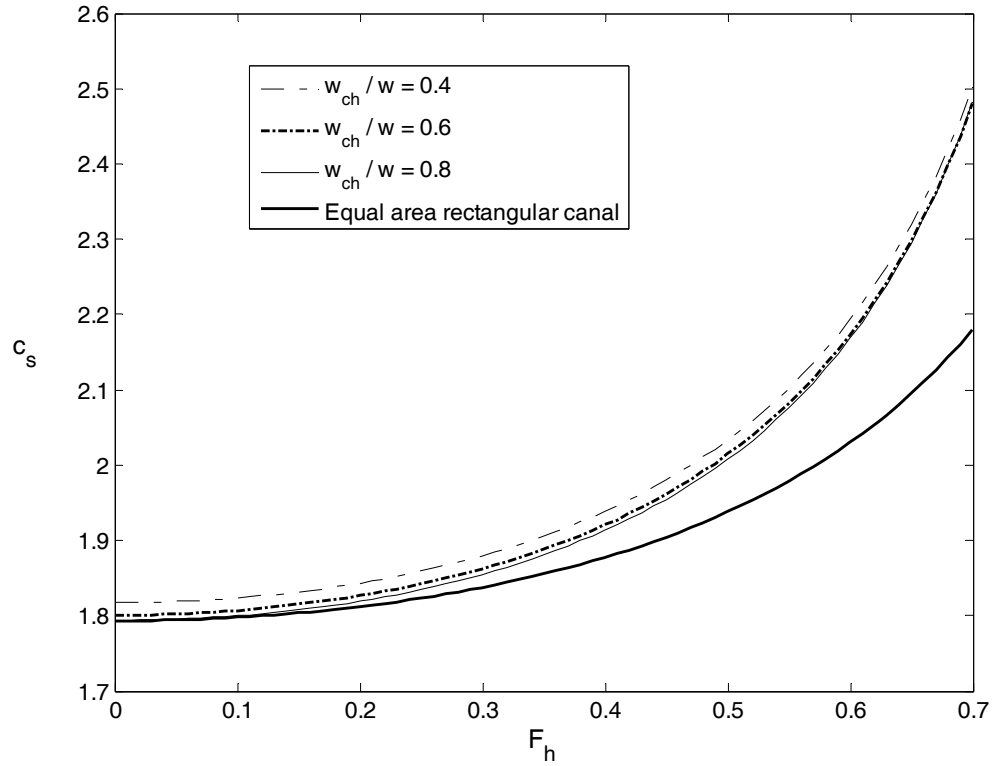

Figure 7: Sinkage coefficient for different channel configurations

We can see that there is very little difference (less than 2%) between the different stepped channel configurations, indicating that different stepped channels tend to produce similar ship squat, provided their waterline width, cross-sectional area and depth at the ship remain constant. This is true whether flow in the outer region is subcritical, critical or supercritical (for this example, flow is supercritical in the outer region for $w_{\mathrm{ch}} / w = 0.8$ and $F_h > 0.5$).

By contrast, results for a rectangular canal with the same cross-sectional area, but different waterline width, vary significantly from the stepped channel configurations at higher Froude numbers (up to 15% at $F_h = 0.7$). This shows that methods using just the channel cross-sectional area, but ignoring the waterline width, may give inaccurate results at higher Froude numbers.

Analysis of equation (21) tells us that, if flow in the outer region is critical ($F_1 = 1$), the solution reduces to that of a canal of width w_{ch}, as happens for the dredged channel case (Section 4). Therefore we can approximate the squat of a ship in a stepped channel by relating this case to a channel of the same waterline width, cross-sectional area and depth at the ship, but with critical flow in the outer region.

It is hypothesized that the squat of a ship travelling along the centreline of a channel of arbitrary cross-section (still assumed roughly symmetric) can also be estimated using this method. The geometry of this method is shown in Figure 8.

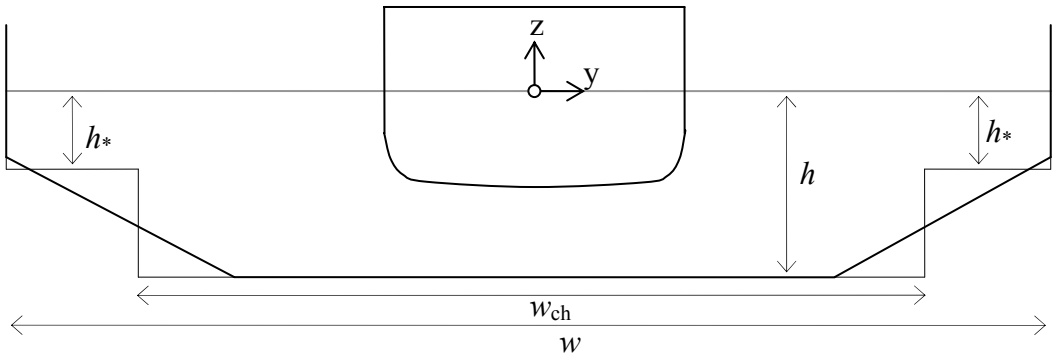

Figure 8: Approximating an arbitrary channel by a stepped depth change with critical flow in the outer section

Suppose we know the waterline width w, cross-sectional area A and depth at the ship h of an arbitrary channel. Then the equivalent stepped channel has inner channel width w_{ch} and outer channel depth h_*. These are found by equating the cross-sectional area:

$$A = w_{ch} h + (w - w_{ch}) h_* \tag{24}$$

and by requiring critical flow in the outer region:

$$\frac{U}{\sqrt{g h_*}} = 1 \tag{25}$$

These can be solved to give

$$\frac{w_{ch}}{w} = \frac{\dfrac{A}{wh} - F_h^2}{1 - F_h^2} \tag{26}$$

This gives an effective channel width

$$w_{eff} = \left[\frac{\dfrac{A}{wh} - F_h^2}{1 - F_h^2} \right] w \tag{27}$$

This effective channel width w_{eff} can be used in the canal formulation (7), giving the approximation for arbitrary canal cross-section

$$Z = -\frac{\rho U^2}{4\pi h \sqrt{1 - F_h^2}} \int_{-\infty}^{\infty} i\, \overline{S'}(k)\, \overline{B^*}(k)\, \coth\left(\frac{w}{2} \left[\frac{\dfrac{A}{wh} - F_h^2}{\sqrt{1 - F_h^2}} \right] k \right) dk \tag{28}$$

9. Summary

We have described a general Fourier transform method for calculating the squat of a ship travelling in open water, a rectangular canal, a dredged channel, a stepped canal or a channel of arbitrary cross-section. The dynamic vertical force is calculated using the following equation:

$$Z = -\frac{\rho U^2}{4\pi h\sqrt{1-F_h^2}} \int_{-\infty}^{\infty} i\,\overline{S'}(k)\,\overline{B^*}(k)\,K(k)\,dk \qquad (29)$$

The bow-down trim moment is found replacing $\overline{B}(k)$ by $\overline{xB}(k)$ in the above equation, and steady sinkage and trim then follow hydrostatically. The function $K(k)$ depends on the transverse geometry, and takes the values

$$K(k) = \begin{cases} \operatorname{sgn}(k) & \text{Open water} \\ \coth\left(\frac{w}{2}\sqrt{1-F_h^2}\,k\right) & \text{Rectangular canal} \\ \dfrac{\cosh\left(\frac{w_{ch}}{2}\sqrt{1-F_h^2}\,k\right) + \frac{h_1\lambda}{h\sqrt{1-F_h^2}\,k}\sinh\left(\frac{w_{ch}}{2}\sqrt{1-F_h^2}\,k\right)}{\sinh\left(\frac{w_{ch}}{2}\sqrt{1-F_h^2}\,k\right) + \frac{h_1\lambda}{h\sqrt{1-F_h^2}\,k}\cosh\left(\frac{w_{ch}}{2}\sqrt{1-F_h^2}\,k\right)} & \text{Dredged channel} \\ \dfrac{\cosh\left(\frac{w_{ch}}{2}\sqrt{1-F_h^2}\,k\right) + \frac{h_1\lambda}{h\sqrt{1-F_h^2}\,k}\sinh\left(\frac{w_{ch}}{2}\sqrt{1-F_h^2}\,k\right)\tanh\left(\lambda(\frac{w-w_{ch}}{2})\right)}{\sinh\left(\frac{w_{ch}}{2}\sqrt{1-F_h^2}\,k\right) + \frac{h_1\lambda}{h\sqrt{1-F_h^2}\,k}\cosh\left(\frac{w_{ch}}{2}\sqrt{1-F_h^2}\,k\right)\tanh\left(\lambda(\frac{w-w_{ch}}{2})\right)} & \text{Stepped canal} \\ \coth\left(\frac{w}{2}\left[\frac{\frac{A}{wh}-F_h^2}{\sqrt{1-F_h^2}}\right]k\right) & \text{Approximation for arbitrary cross section} \end{cases} \qquad (30)$$

10. References

Beck, R.F., Newman, J.N. & Tuck, E.O. 1975 Hydrodynamic forces on ships in dredged channels. Journal of Ship Research 19(3), 166 – 171.

Dand, I.W. & Ferguson, A.M. 1973 The squat of full ships in shallow water. Trans. RINA 115, 237 – 255.

Gourlay, T.P. 2006 Flow beneath a ship at small underkeel clearance. Journal of Ship Research 50(3), 250 – 258.

Gourlay, T.P. & Tuck, E.O. 2001 The maximum sinkage of a ship. Journal of Ship Research 45(1), 50 – 58.

Gourlay, T.P. 2000 Mathematical and computational techniques for predicting the squat of ships. Ph.D. thesis, University of Adelaide.

Michell, J.H. 1898 The wave resistance of a ship. Phil. Mag. (5), Vol. 36, 430 – 437.

Roseman, D.P. (Ed.) 1987 The MarAd systematic series of full form ship models. SNAME publications.

Sharma, S. D. & Chen, X.-N. 2000 Interaction of ship waves with river banks and uneven bottom. Proceedings, 4th International Conference on Hydrodynamics, Yokohama, 157.

Tuck, E.O. 1964 A systematic asymptotic expansion procedure for slender ships. Journal of Ship Research 8, 15 – 23.

Tuck, E.O. 1966 Shallow water flows past slender bodies. Journal of Fluid Mechanics 26, 81 – 95.

Tuck, E.O. 1967 Sinkage and trim in shallow water of finite width. Schiffstechnik 14, 92 – 94.